Geometry Pumping on Spacecraft
(The CFE-Vane Gap Experiments on ISS)

M.M. WEISLOGEL[1], R.M. JENSON[1], Y. CHEN[1], S.H. COLLICOTT[2], and S. WILLIAMS[3]

[1] Portland State University, Portland, USA, me_dept@cecs.pdx.edu
[2]Purdue University, West Lafayette, USA, collicot@purdue.edu
[3]NASA Johnson Space Center, Houston, USA, sunita.1.williams@jsc.nasa.gov

Abstract

Current experiments aboard the International Space Station (ISS) illustrate an extent to which liquid behavior aboard spacecraft can be controlled by wetting and container geometry. The experiments are referred to as the 'Vane-Gap' experiments and are part of a more general set of simple handheld Capillary Flow Experiments[1)] (CFE) designed and developed at NASA's Glenn Research Center for conduct on ISS. The CFE-Vane Gap experiments highlight the sensitivity of a capillary fluid surface to container shape and how small changes to said shape may result in dramatic global shifts of the liquid within the container. Understanding such behaviors is central to the passive management of liquids aboard spacecraft and in certain cases permits us the ability to move (pump) large quantities (potentially tons) of liquid by a simple choice of container shape. In particular, the Vane-Gap experiments identify the critical geometric wetting conditions of a vane structure that does not quite meet the container wall—a construct arising in various fluid systems aboard spacecraft such as liquid fuel and cryogen storage tanks, thermal fluids management, and water processing equipment. In this paper experimental results are compared with preliminary theoretical and numerical analyses.

1. Introduction

The CFE-Vane Gap experiments[1)] are the latest of a line of experiments performed in low-g environments and sponsored by NASA to observe critical corner wetting phenomena in large length scale capillary systems[2-5)]. Mathematicians Concus and Finn[6)] were perhaps first to identify the mathematical foundations of the critical interior corner wetting condition that, if satisfied, spontaneously draws the liquid into and along the corner to an impressive extent. The wetting condition is given by the simple relation $\theta < \pi/2 - \alpha$, where θ is the wetting angle of the liquid on the solid surface and α is the corner half-angle. Such critical wetting conditions dictate the design of systems seeking to exploit the passive pumping capacity of the interior corner geometry.

As container geometry becomes increasingly complex the critical geometric wetting criteria becomes significantly more complicated. For example, an intricate geometric wetting condition arises for interior corners that do not actually contact. Such conditions are present in certain spacecraft propellant tanks where a gap is formed between a vane and the tank wall as sketched in **Fig. 1**. The CFE-Vane Gap experiments are devised to investigate such phenomena and provide a benchmark to both confirm and guide methods of design for systems of increased complexity. The long duration (~hours) low-g environment of the International Space Station (ISS) is ideal for such sensitive, large length scale capillary experiments.

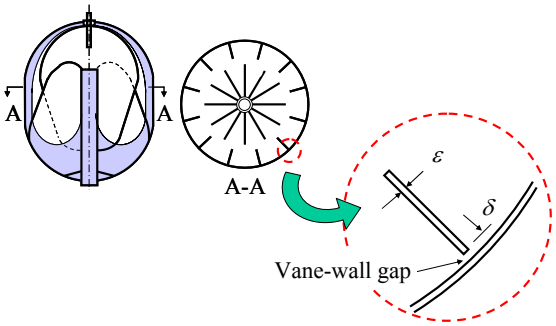

Fig. 1 Sketch of model spacecraft fuel tank with internal vanes[7)]; liquid over liquid exit, vapor over vapor exit.

2. Hardware and Experiments

An image, schematic, and test cell cross section of a Vane Gap test unit is shown in **Fig. 2**. The test unit employs a right cylinder with elliptic cross section and a single central vane that does not contact the container walls. The vane rotates which serves two purposes: to vary the angle between the vane and wall and at the same time vary the size of the vane-wall gap. The vane is also slightly asymmetric so that two gaps can be tested for each container. Two wetting conditions are studied between the two Vane Gap containers: one exhibits a perfect wetting situation (VG-1) with $\theta \approx 0°$ and the other exhibits a partially wetting condition with $\theta = 55°$ (VG-2). The units are identical in every aspect except wetting condition and vane dimensions. Some details are listed below:

1. Ellipse Section: 50.8 by 33.9mm.
2. Height is 127mm.

3. Large Bond number limit, Bo >> 1 (i.e. 1-g, flat surface), liquid fill level is 38.1mm from base.
4. Vane dimensions:
   VG-1—31.3 by 2.0 by 114.3mm
   VG-2—31.3 by 5.0 by 114.3mm.
5. The vane rotation axis is coaxial with the ellipse but the gap dimensions are 0.838 and 1.676mm when vane is aligned along the minor diameter of ellipse. These gap dimensions represent a 0.05 and 0.1 dimensionless gap using the minor axis radius for normalization.
6. Vane angle rotation ±360º ±1º resolution
7. Contact angles are ≈ 55º ± 5º (VG-2, FC724 coating) and 0º (VG-1, no coating).
8. Liquid is 10cs Si Oil.
9. Liquid volume is 49.1cc.

Preliminary experimental results are presented herein primarily for VG-1, where $\theta = 0º$.

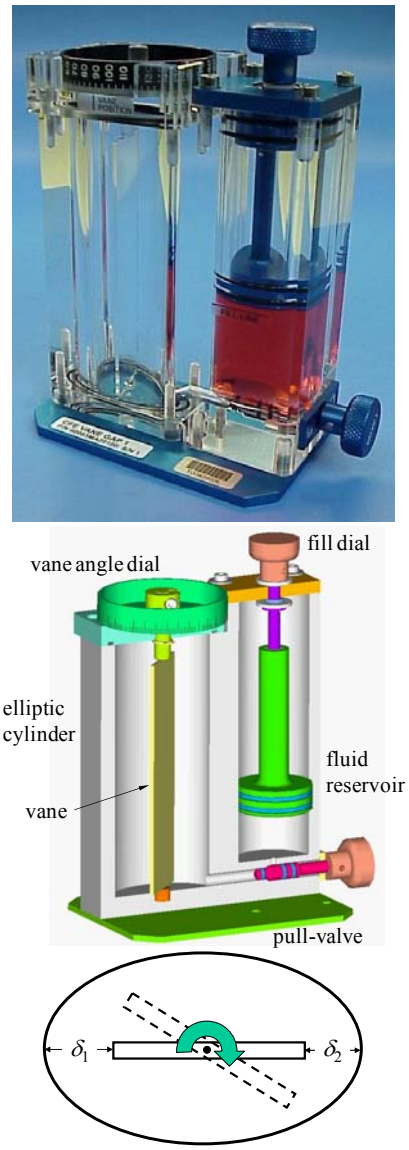

Fig. 2 CFE Vane Gap Flight Unit: Image, schematic, and cross-section. (Vane angle rotates ±360º)

The crew procedures and experiment objectives are reviewed here with reference to Figs. 2 and **3**. The Maintenance Work Area (MWA, a 'portable work bench') of the ISS is used as the platform on which to conduct the experiments. The test unit is mounted to the surface of the MWA using a single captive fastener. An ISS camcorder is positioned normal to the front face of the test vessel and a sheet of paper is employed as a diffuse backlight screen. The experimental procedures consist of pulling open the valve, dispensing the liquid from the reservoir into the test section, and then adjusting the vane angle dial to various pre-determined positions listed in the crew procedures available to the crew on an ISS laptop computer.

As sketched in Fig. 2, the vane can be rotated changing both the vane-wall angle and the vane-wall gap size. At a critical vane angle the fluid spontaneously wets one of the 'gapped corners' and rises to the top of the vane at which point the vane angle is determined for comparison to predictions.

The vane is slightly asymmetric so that two 'gaps' can be tested for each container. An initial +360º rotation (consider an 'initially dry test') is followed by two repeat +360º tests (considered 'wet test'). These tests identify the critical angles and time response of the fluid such that fixed angle and wait times can be specified with greater precision. Two -360º revolutions are then conducted to identify hysteresis in the measurements. For both CFE-VG vessels critical wetting angles are determined to ±1º with transient fluid reorientations requiring between 3 to 15 minutes for equilibration. The static and dynamic interface profiles are recorded by an ISS camcorder. Real-time and video dump footage is available for immediate comparisons with predictions. The flight tapes are returned to Earth at the earliest opportunity and many such tapes are currently in the possession of the authors.

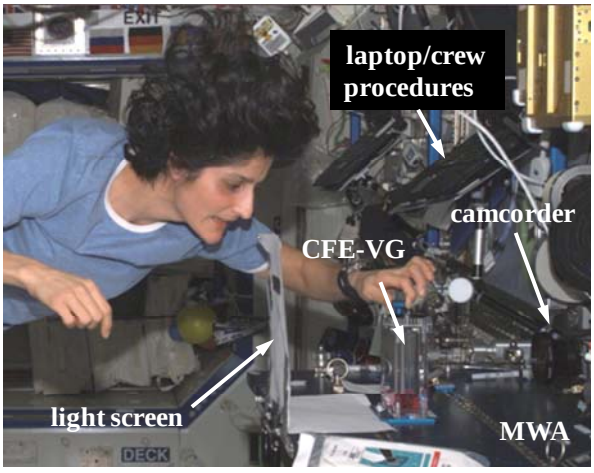

Fig. 3 Experimental setup for CFE-VG on ISS.

3. Preliminary Results

Sample images of preliminary 'near-equilibrium states' captured during the flight operations of the experiment are presented in **Figs. 4 and 5**. They are labeled 'near-equilibrium' because they are results from the first operation of the experiment. Subsequent operations established equilibrium conditions with a degree of certainty not present here. The latter will be published in a subsequent article once the complete data set is received and analyzed.

The behavior of the fluid is obvious and subcritical static interfaces are shown for vane angles 0º and 30º, while large and small gap critical wetting conditions are shown at 44º and 60º, respectively (Fig. 4). Large and small gap de-wetting occurs at vane angles 130º and 138.5º, respectively (Fig. 5), with a return to subcritical surfaces at vane angles 150º and 180º.

Numerical predictions of the surface behavior using the *Surface Evolver* algorithm[8] and oringinally specified contact angle $\theta = 60º$ were carried out prior to conduct of the experiments for engineering design purposes. These images are presented beneath each photo in Figs. 4 and 5 to the nearest 5º (computed vane angle provided in parenthesis where different from experiment). It is clear that the predictions are at least qualitatively correct. However, it is also clear that a global shift in the liquid occurs for certain critical vane angles which was not at all captured by the initial design numerical predictions (see vane angles 60, 90, 126, 130, and 138.5º). The global reorientation requires as much as 15 minutes to complete and is nearly imperceptible to the observer (i.e. the crewmember conducting the experiment). Such lengthy reorientation times testify to the small driving forces present, or, in the case of the numerical solutions, small surface energy gradients. The influence of background accelerations is ruled out due to insufficient magnitude and direction. Following observations of the global shift, subsequent computations have been able to replicate it, but only in hindsight and after abnormally deep convergence. The global shift is only observed for the $\theta = 0º$ Vane Gap vessel (CFE-VG-1) and not for the $\theta \approx 55º$ vessel. The fact that the global shift was not observed for the $\theta \approx 55º$ Vane Gap vessel (CFE-VG-2) is currently attributed to contact angle hysteresis $\approx \pm 5º$ which is capable of resisting the minute capillary forces present at such near-critical geometric wetting conditions.

The global shift is computed analytically using the general approach of Concus and Finn[9-11]. The three conditions (sections) are depicted in **Fig. 6**. In all cases the critical analytically-determined vane angles are such that $\phi_1 < \phi_3 < \phi_2$. From the experiments it is certain that $\phi_1 < \phi_2$. However, ϕ_3 could be $\phi_1 < \phi_3 < \phi_2$, or $\phi_3 < \phi_1 < \phi_2$—varying within quadrants of the same cell. This means that the global shift could be observed to occur with or without critical gap wetting (not shown in Figs. 4 and 5).

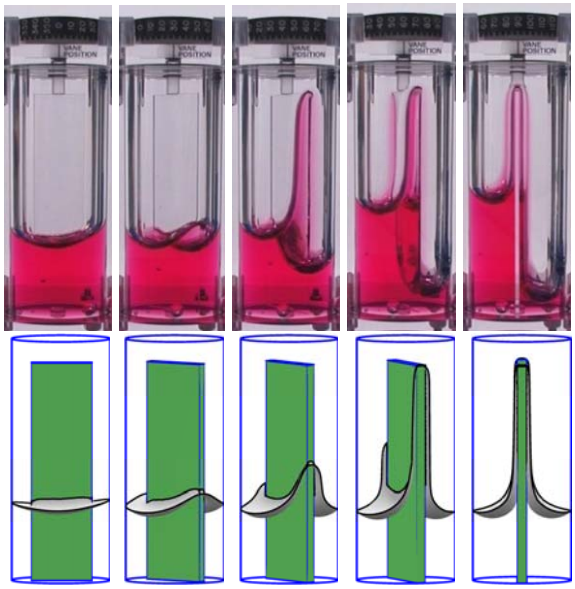

Fig. 4 Images of interface states (computations) at vane angles 0, 30, 44 (45), 60, and 90º.

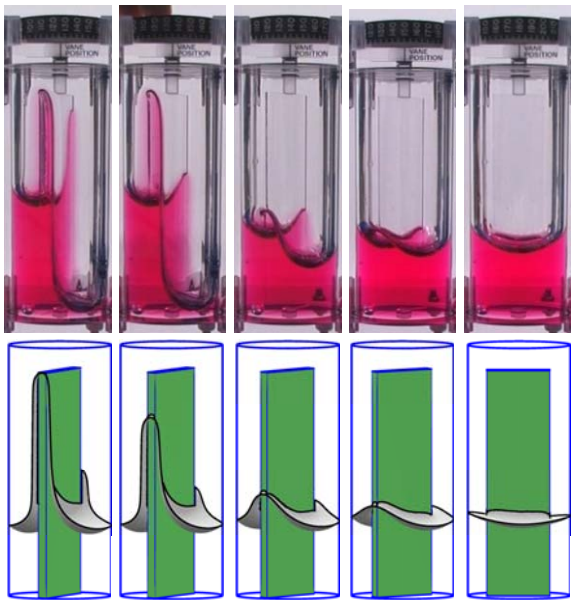

Fig. 5 Images of interface states (computations) at vane angles 126 (125), 130, 138.5 (140), 150, and 180º.

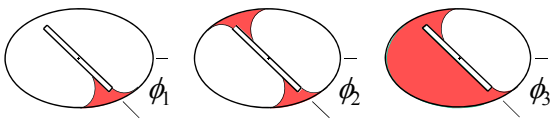

Fig. 6 Theoretical critical wetting configurations.

The wetting dynamics are also different for critical gap de/wetting and bulk de/wetting flows. In **Fig. 7** an image of the test cell CFE-VG-1 is provided identifying three key locations L_1, Z_1, and Z_2 on the interface that are tracked for the purposes of this presentation. This specific case is for the advancing meniscus location for the narrow gap wetting event (Fig. 4, 44º), the dynamics

of which are digitized and plotted in **Fig. 8**. L_1, Z_1, and Z_2 denote the advancing tip, advancing bulk meniscus, and receding bulk meniscus, respectively. The data for L_1, Z_1, and Z_2 are also plotted in Fig. 8 against $t^{3/4}$, where a strong linear trend is observed. (It should be noted that $L_1 - Z_1$ and $L_1 - Z_2$ are both linear with $t^{3/4}$.)

The advancing meniscus for a pure bulk shift event (case where there is no critical wetting of the gapped corners—not pictured in Figs. 4 and 5) is plotted in Fig. 9 against t, where the flattening of the data at large time, t > 150s, is due to finite container size affects. The linearity of both curves (Fig. 8 where $L_1 \sim t^{3/4}$ and **Fig. 9** where $Z_1 - Z_2 \sim t$) demonstrates convincingly that different mechanisms are responsible the different transients. The latter behavior is presently attributed in part to slight asymmetries in the container shape and will be further pursued both theoretically and numerically. (The accumulative vane axis tolerance is < ±0.1mm over container section dimensions of 50.8 by 33.9mm.)

Lastly, a third wetting dynamic is observed in the flight experiments where the vane gap is de/wetted without a global shift in the fluid. In such cases $L_1 \sim t^{1/2}$ is observed as is common in short duration drop tower experiments for sharp[12] as well as gapped corner geometries[13]. These and other data will be discussed in greater detail in a subsequent article.

4. Summary of Observations and Impact

Critical vane gap wetting, as demonstrated by the flight experiments in Figs. 4 and 5, is dependent on the vane angle and fluid wetting properties (ϕ and θ), similarly as for ideal sharp corners[6], but also by the additional geometric effects of the specific vane gap, vane thickness, container size and shape, and even time.

As might be expected, the dynamics of the wetting process are also complicated by the geometry. As observed in Figs. 8 and 9 different geometric mechanisms for the different critical wetting conditions produce different time dependencies for the resulting flows. Analyses of the dynamics for such problems are capable of predicting the essential transients of these events as functions of the specific geometry and will be reported subsequently along with the complete experimental data set and concurrent analyses.

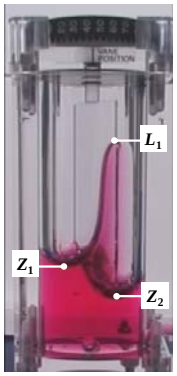

Fig. 7 Notation for wetting dynamics

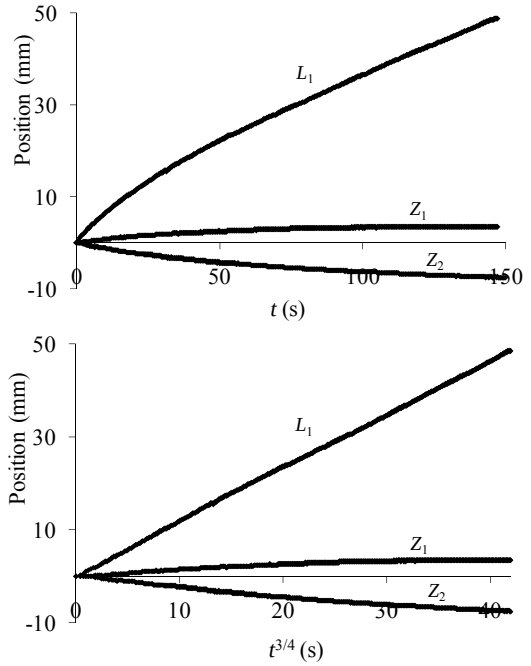

Fig. 8 Typical vane gap wetting dynamics (Fig. 4, 44º): $L_1(t)$ and $L_1(t^{3/4})$.

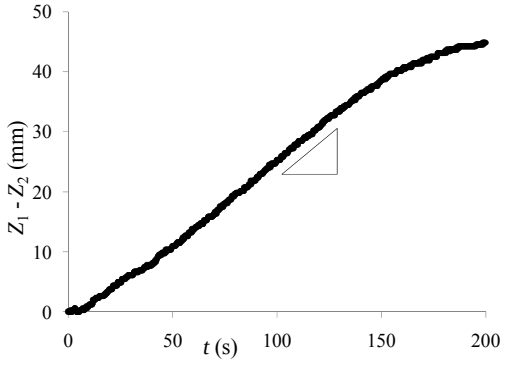

Fig. 9 Typical bulk shift wetting dynamics: $Z_1 - Z_2$ vs. t.

Concerning applications, and in concert with previous investigations, it is evident that fluids may be positioned and/or otherwise controlled as desired by simply and slightly changing the geometry of container. For example, for the CFE-VG-1 test unit, a 1º rotation of the vane produces a global shift of the fluid from one side of the container (i.e. the base) to another (i.e. the side wall). Conversely, knowledge of such critical geometric wetting behavior might avoid mishaps. For example, a slight but uncontrolled container asymmetry might lead to a highly unfavorable shift in fluid preventing or limiting system function. As a precaution against such surprises, sensitivity analyses for interfaces near critical wetting conditions should be performed as a function of design tolerances.

The CFE Vane Gap experiments may provide a means for specifying container tolerance as a function of system geometry and wettability. The experiments also provide a unique benchmark for static and dynamic

geometric wetting phenomena common to complex capillary systems in space and on Earth.

Acknowledgements

The authors wish to thank crewmembers J. Williams and C. Anderson and the NASA cadre at Glenn Research Center, Marshall Space Flight Center, and Johnson Space Flight Center.

References

1) Weislogel, M.M., Collicott, S.H., Gotti, D.J., Bunnell, C.T., Kurta, C.E. and Golliher, E., The Capillary Flow Experiments: Handheld Fluids Experiments for the International Space Station, AIAA 2004-1148, 42nd AIAA Aerospace Sci. Meeting, Reno, NV 5-8, Jan. 2004.
2) Concus, P. and Finn, R., Capillary Surfaces in Microgravity, in "Low-Gravity Fluid Dynamics and Transport Phenomena," **130**, Progress in Astronautics and Aeronautics, AIAA, 183-204 1990.
3) Concus, P., Finn, R. and Weislogel, M., Capillary Surfaces in an Exotic Container: Results from Space Experiments, *J. Fluid Mech*. **394**, 119-135, October 1999.
4) Concus, P., Finn, R. and Weislogel, M., Measurement of Critical Contact Angle in a Microgravity Experiment, *Experiments in Fluids*, **28**:3, 197-205, 2000.
5) Langbein, D., Capillary Surfaces: "Shape-Stability-Dynamics, in Particular under Weightlessness," Springer Tracts in Modern Physics, **178**, 2002.
6) Concus, P. and Finn, R., On the Behavior of a Capillary Free Surface in a Wedge, *Proc. Nat. Acad. Sci*., USA, **63**:2, 292-299, June 1969.
7) Chato, D.J. and Martin, T.A., Vented Tank Resupply Experiment—Flight Test Results, 33rd AIAA/ASME/SAE/ASEE Jnt. Propulsion Conf., AIAA-97-2815, July 6-9, Seattle 1997.
8) K.A. Brakke, *Surface Evolver* program, available at http://www.susqu.edu/facstaff/b/brakke/, (code and manual).
9) Finn, R., A Subsidiary Variational Problem and Existence Criteria for Capillary Surfaces*, J. Reine Angew. Math*., **353**, 196-214, 1984.
10) Chen, Y. and Collicott, S.H., Investigation of the symmetric wetting of vane-wall gaps in propellant tanks, *AIAA J*., **42**, 2, 305-314, 2004.
11) Chen, Y. and Collicott, S.H., Study of wetting in an asymmetrical vane-wall gap in propellant tanks, *AIAA J*., **44**, 4, 859-867, 2006.
12) Weislogel, M.M. and Lichter, S., Capillary Flow in Interior Corners, *J. Fluid Mech*., **373**, 349-378, November 1998.
13) Chen, Y. and Collicott, S.H., Experimental study on capillary flow in a vane-wall gap geometry, *AIAA J*., **43**, 11, 2395-2403, 2005.